NANO LETTERS

xxxx
Vol. 0, No. 0
A−F

In situ Control of Atomic-Scale Si Layer with Huge Strain in the Nanoheterostructure NiSi/Si/NiSi through Point Contact Reaction

Kuo-Chang Lu,[†,||] Wen-Wei Wu,[‡,||] Han-Wei Wu,[‡] Carey M. Tanner,[§] Jane P. Chang,[§] Lih J. Chen,[*,‡] and K. N. Tu[*,†]

Department of Materials Science and Engineering, Department of Chemical and Biomolecular Engineering, University of California, Los Angeles, Los Angeles, California 90095-1595, and Department of Materials Science and Engineering, National Tsing Hua University, Hsinchu 300, Taiwan, Republic of China

Received May 3, 2007; Revised Manuscript Received June 18, 2007

ABSTRACT

Nanoheterostructures of NiSi/Si/NiSi in which the length of the Si region can be controlled down to 2 nm have been produced using in situ point contact reaction between Si and Ni nanowires in an ultrahigh vacuum transmission electron microscope. The Si region was found to be highly strained (more than 12%). The strain increases with the decreasing Si layer thickness and can be controlled by varying the heating temperature. It was observed that the Si nanowire is transformed into a bamboo-type grain of single-crystal NiSi from both ends following the path with low-activation energy. We propose the reaction is assisted by interstitial diffusion of Ni atoms within the Si nanowire and is limited by the rate of dissolution of Ni into Si at the point contact interface. The rate of incorporation of Ni atoms to support the growth of NiSi has been measured to be 7×10^{-4} s per Ni atom. The nanoscale epitaxial growth rate of single-crystal NiSi has been measured using high-resolution lattice-imaging videos. On the basis of the rate, we can control the consumption of Si and, in turn, the dimensions of the nanoheterostructure down to less than 2 nm, thereby far exceeding the limit of conventional patterning process. The controlled huge strain in the controlled atomic scale Si region, potential gate of Si nanowire-based transistors, is expected to significantly impact the performance of electronic devices.

As the end of the semiconductor roadmap approaches for very large scale integration of Si-based field effect transistors, the development of nanoscale transistors based on Si nanowires is of wide interest for their applications in electronics industry and life sciences.[1−3] To realize this potential, the formation of silicide nanowires, either by substrate growth[4−7] or by free-standing growth,[8−12] and nanowire heterostructures has been investigated.[4,5,13,14] Wu et al. created NiSi/Si nanowire heterostructures.[4] The single-crystal NiSi nanowires have ideal resistivities and remarkably high failure current densities. Field-effect transistors were fabricated based on those heterostructures in which the source−drain contacts are defined by the metallic NiSi nanowire regions.[4] Weber et al. fabricated Schottky barrier field effect transistors based on similar heterostructures and characterized with respect to their gate lengths.[5] On the other hand, how to achieve a precisely controlled nanostructure remains one of the most challenging problems in nanotechnology today. In this work, we report a novel method to fabricate the heterostructures utilizing in situ point contact reaction between Ni and Si nanowires in a high-resolution transmission electron microscope (TEM). The growth kinetics of Ni silicide in nanoscale, which we found to be distinctly different from that in thin films, has become very important. In situ TEM is a powerful tool[6,15−24] for the study on growth kinetics. Our method allowed us to study the growth process and reaction mechanism and thereby to control the dimension of the Si region, the potential gate of a Si nanowire transistor,[5] down to atomic scale around one order smaller than the current state-of-art knowledge. Also, the huge strain in the Si region can be controlled, which shall be beneficial in the development of high-performance sub-10 nm silicon devices.[25,26]

The monosilicide NiSi was selected because of its low resistivity for applications in shallow junction devices.[27]

* To whom correspondence should be addressed. E-mail: (L.J.C.) ljchen@mx.nthu.edu.tw; (K.N.T) kntu@seas.ucla.edu.

† Department of Materials Science and Engineering, University of California, Los Angeles.

‡ Department of Materials Science and Engineering, National Tsing Hua University.

§ Department of Chemical and Biomolecular Engineering, University of California, Los Angeles.

|| These authors contributed equally to this work.

10.1021/nl071046u CCC: $37.00
Published on Web 06/30/2007

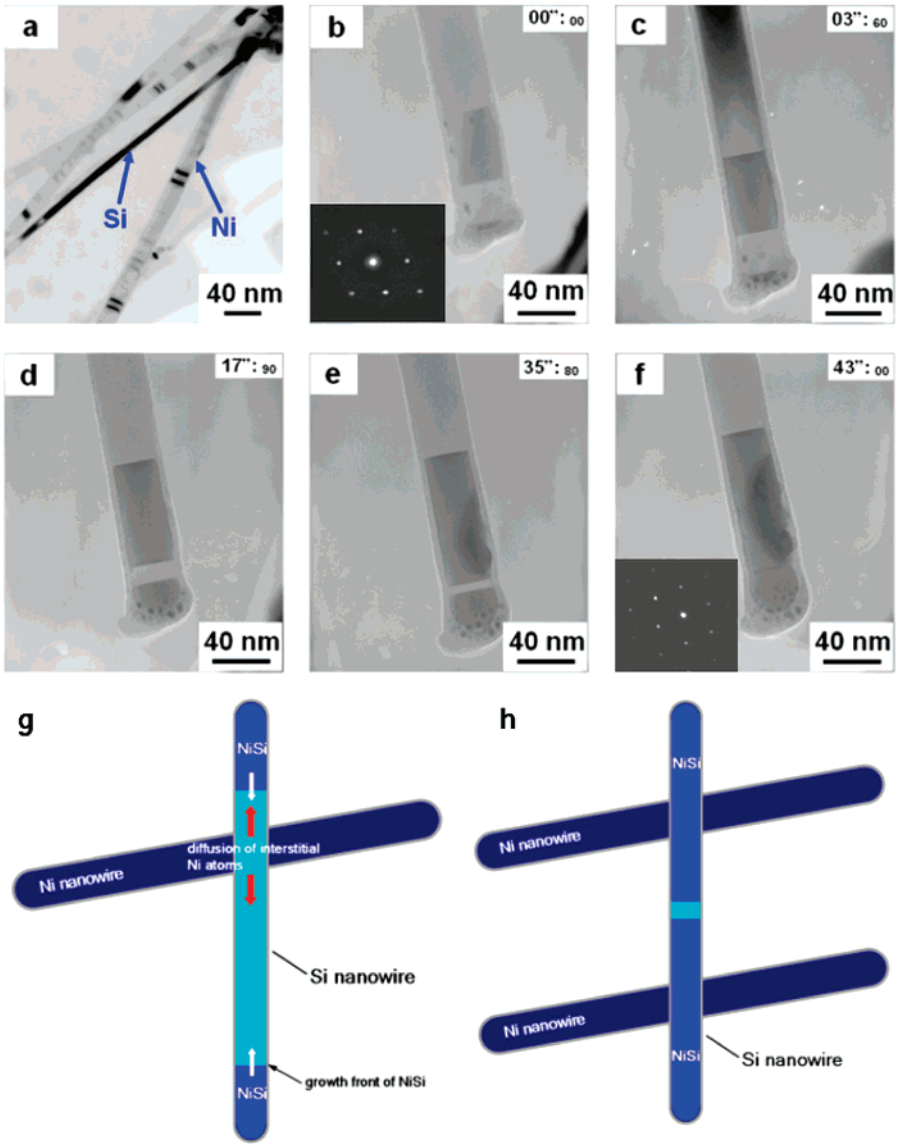

Figure 1. Overview of NiSi formation within Si nanowires by point contact reaction. (a) A TEM image of Si and Ni nanowires dispersed on a Si_3N_4 membrane. (b−f) Sequence of in situ TEM images depicting the growth of a bamboo-type grain of NiSi within a Si nanowire at 700 °C. (b, inset) Selected area diffraction pattern with [1−10] zone axis of Si. (f, inset) Selected area diffraction pattern with [1−12] zone axis of NiSi. The time of the image capture is given in the rectangular box at the upper-right corner. The first two numbers are in units of seconds and the following two smaller numbers are in units of 1/100 s. (g) A schematic illustration of NiSi growth within a Si nanowire. (h) A schematic illustration of growth of a NiSi/Si/NiSi heterostructure where the length of the Si section is controlled at the atomic scale.

Epitaxial Ni silicide formation in thin film reactions has been studied.[28−33] In point contact reactions between Ni and Si nanowires, we have observed reactive epitaxial growth of NiSi on Si in which the epitaxial interface is moving. The growth rate is determined as a function of time and temperature, and the activation energy is calculated. A mechanism of such dynamic epitaxial growth is proposed. As a result, we are able to tailor the NiSi growth by stopping the reaction prior to complete consumption of the Si nanowire, thereby controlling the remaining length of the Si region down to atomic scale. Thus, we fabricate a series of heterostructures of NiSi/Si/NiSi with varying Si length from 2 to 200 nm. The interfaces between the Si and NiSi are atomically flat, and the growth is epitaxial.

Silicon nanowires were prepared on a p-type Si wafer by the vapor−liquid−solid method using Au nanodots as nucleation sites for single-crystal Si nanowires with a [111] growth direction.[34,35] Ni nanowires were synthesized via the anodic aluminum oxidation method and were stored in isoproponal.[36] The Ni nanowires and Si nanowires ranged in diameter from 10 to 40 nm with lengths of a few microns.

To prepare point contact samples, we drip droplets of both solutions on Si grids with a square opening covered with a window of a glassy Si_3N_4 film. The thickness of the Si_3N_4 film is about 20 nm so that it is transparent to the electron beam and does not interfere with the imaging of the nanowires. The samples were dried under light bulbs. Figure 1a shows a typical TEM image of randomly oriented Si and Ni nanowires on the window prior to annealing. Both the Si and Ni nanowires are single crystal with a thin surface oxide (∼1−5 nm thick). Darker contrast appears on the Si

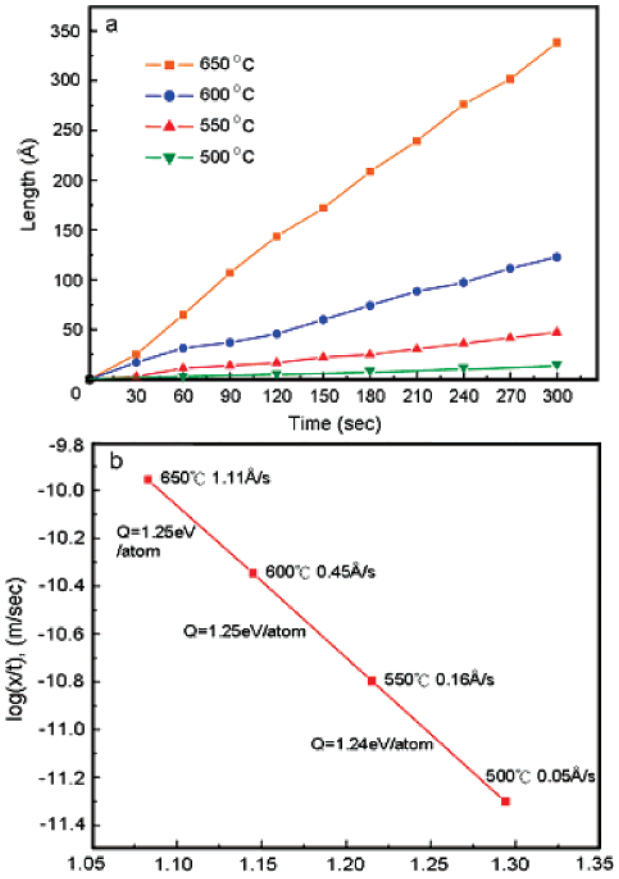

Figure 2. Kinetic analysis of the NiSi epitaxial growth within a Si nanowire of 20 nm in diameter. (a) Plot of the NiSi nanowire length vs reaction time at various temperatures, illustrating a linear growth rate. The lines are drawn as guides. (b) Arrhenius plot of the NiSi epitaxial growth from which the activation energy was determined.

nanowire, resulting from the fact that the zone axis is accurately parallel to Si [110].

Most of our experiments on in situ annealing for point contact reactions were conducted in a JEOL 2000V ultrahigh vacuum TEM where the sample can be heated to 1000 °C, and the vacuum in the sample stage is about 3×10^{-10} Torr. High-resolution lattice images were also taken in a JEOL 3000F high-resolution TEM (HRTEM), and the vacuum in the sample stage is better than 10^{-6} Torr.

Figure 1b−f shows a time-lapsed series of in situ TEM images capturing the growth of a bamboo-type NiSi grain within a straight Si nanowire at 700 °C. On the basis of the HRTEM images and selected area diffraction patterns, we determined the structure of the material to be single-crystal NiSi.

Figure 1g is a schematic diagram depicting the growth of NiSi in which the Ni atoms dissolve and diffuse interstitially in Si[37] and stop at the ends of the Si nanowire, thereby nucleating growth of NiSi to form a NiSi/Si/NiSi heterostructure. Some Ni atoms may be able to diffuse through a grain of silicide; hence, we observed additional and smaller silicide growth at the tip, which is attached to the main silicide at the end. Figure 1h depicts two Ni nanowires making contacts to a Si nanowire in which the NiSi grains have passed the point contacts requiring the Ni atoms to diffuse through the NiSi.

To determine the growth kinetics of NiSi in Si nanowires, we conducted dynamic observation in real time using in situ TEM video. The atomic-scale microstructures were recorded over time, allowing us to obtain lattice images of the progression of the atomically flat epitaxial interfaces. Movie 1 in Supporting Information shows the growth of a single-crystal NiSi nanowire within a Si nanowire at 10 times the actual speed.

Figure 2 shows the linear growth behavior of the NiSi nanowire in the Si nanowire of 20 nm in diameter over the temperatures ranged from 500 to 650 °C. The activation energy of the epitaxial growth was determined to be 1.25 eV/atom, compared to the activation energy of interstitial diffusion of Ni in Si of about 0.47 eV/atom,[38] indicating that the growth may be interface reaction controlled.

Figure 3a−c shows a set of HRTEM images of the NiSi/Si interface taken as the interface advances into the Si. The interface is parallel to the (111) plane of Si as well as the (311) plane of NiSi. Thus, the growth direction of NiSi is normal to the (311) plane. The crystallographic orientation relationships between Si and NiSi, which has an orthorhombic lattice with lattice constants of $a = 0.562$ nm, $b = 0.518$ nm, and $c = 0.334$ nm,[39] are

$$[1\bar{1}\,0]\mathrm{Si} \,//\, [1\bar{1}\,2]\mathrm{NiSi}, \text{ and } (111)\mathrm{Si} \,//\, (31\bar{1})\mathrm{NiSi}$$

Across the epitaxial interface, the misfit on the basis that the interplanar spacing of Si (111) and twice NiSi (131) are 0.31355 and 0.29594 nm, respectively, is

$$f = \frac{d_{\mathrm{Si}} - d_{\mathrm{NiSi}}}{d_{\mathrm{Si}}} = \frac{0.31355 - 0.29594}{0.31355} = \frac{0.01761}{0.31355} \cong 5.62\%$$

If misfit dislocations exist, the spacing between them should be about 18×0.31 nm $= 5.58$ nm, which is smaller than the ~20 nm diameter of the Si nanowire. However, we were unable to find any misfit dislocations at the NiSi/Si epitaxial interface, and this may be because of the difficulty in nucleation of the dislocations in a perfect nanowire.[40] Movie 2 in Supporting Information shows the growth of the NiSi/Si epitaxial interface within a Si nanowire in high resolution.

Figure 3d−f shows another set of HRTEM images of the growth of an epitaxial interface of NiSi/Si containing a large step of about 3 nm along the (111) plane of Si. The (111) Si planes are replaced by the (131) planes of NiSi as the interface advances. Knowing the diameter of the wire and the growth rate, we can estimate the total number of Ni atoms in a given volume of the wire based on the unit cell volume of NiSi and the number of Ni atoms per unit cell. Thus, we have determined that for growth at 700 °C the time needed to incorporate one Ni atom on the growth interface is about 7×10^{-4} sec. The value is the same for the two sets of epitaxial growth shown in Figure 3. At lower growth temperatures, the growth rate is slower, and we can achieve

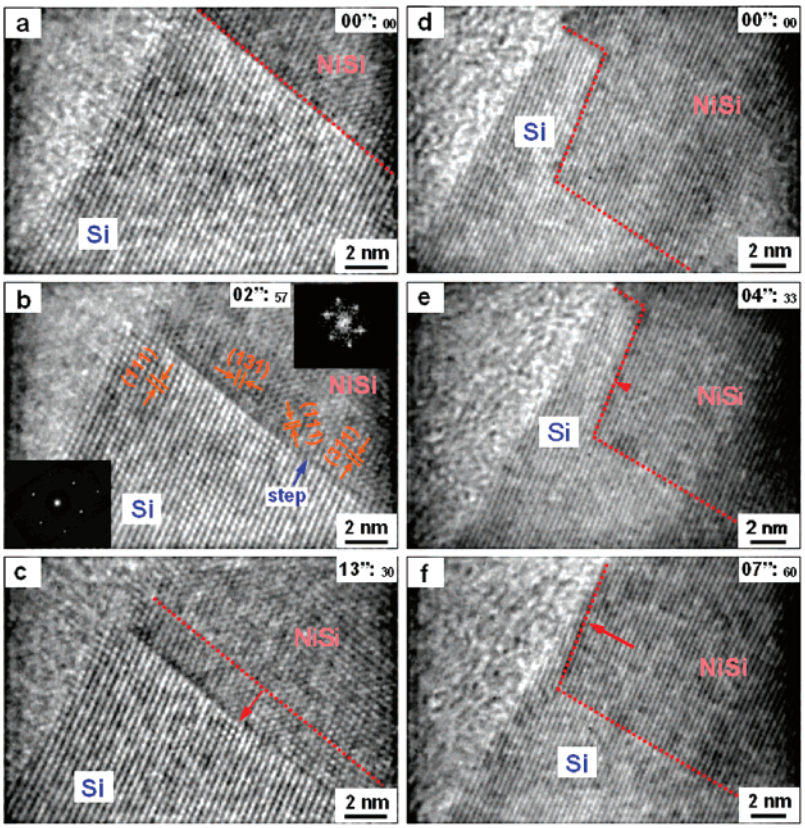

Figure 3. In situ HRTEM image sequences of the growing NiSi/Si epitaxial interfaces within Si nanowires. (a−c) In situ HRTEM image sequence of the growth of the NiSi/Si epitaxial interface. From (a−c) growth of 5 atomic layers has occurred, as indicated by the arrow in (c). The insets in (b) are the corresponding selected area diffraction pattern with [1−10] Si zone axis and fast Fourier transform (FFT) pattern confirming the [1−12] NiSi zone axis, respectively. (d−f) In situ HRTEM image sequence of a moving NiSi/Si epitaxial interface with a large step. The time of the image capture is given in the rectangular box at the upper-right corners. The first two numbers are in units of seconds and the following two smaller numbers are in units of 1/100 s. For (d−f), growth of 10 atomic layers has occurred. The length of the red arrow in (f) indicates the number of layers grown between **(**d) and (f).

control of single atomic layer growth. Movie 3 in Supporting Information shows the growth of the NiSi/Si epitaxial interface with a large step within a Si nanowire in high resolution.

We can estimate the time for Ni atoms to diffuse in a Si nanowire from $x^2 = Dt$ where x is the length of the Si nanowire between the point contact and the Si/silicide interface, D is interstitial diffusivity of Ni atoms in Si nanowires, and t is the time. If we take D to be 10^{-6} cm^2/sec and x to be 1 μm, we have $t = 10^{-2}$ s.[37] Because the diffusion time is much longer than what was estimated for the growth of one atom on the epitaxial interface, the growth cannot be interfacial reaction controlled at the epitaxial interface. Instead, we propose that the reaction may be limited by the rate of dissolution of Ni into Si at the point contact interface. Atomic flux by definition is the number of atoms per unit area and per unit time, so that the number of Ni atoms diffusing into Si is equal to flux times area times time.[32] If the contact area is very small, the number of Ni atoms diffusing into Si will be extremely small. As a result, the reaction is limited by how fast the Ni atoms can diffuse into the Si nanowire or how large the Ni flux is. This is a unique feature of point contact reactions. A diameter dependence on the axial growth rate, that is, nanowires (NWs) of smaller diameter showing greater growth rate, was found. The result also suggests that the rate-limiting step is indeed transport of Ni through the SiO_2 shell. Surface diffusion of Ni on the SiO_2 surface of the Si nanowire was considered; however, it is slower than the interstitial diffusion of Ni within Si,[37,41] which dominates the reactions.

Figure 1g depicts the growth of NiSi from both ends of a Si nanowire. It leads to the formation of a NiSi/Si/NiSi nanoheterostructure as shown in Figure 4a,b. The darker regions at the two ends are NiSi, and the lighter region in the middle is Si. Silicide formation occurs at both ends of the Si nanowire, as shown in Movie 4 in Supporting Information, and if annealing is stopped before the entire nanowire transforms into NiSi, as in Figure 4c, a nanoheterostructure is formed as shown in Figure 4a,b. Often, the growth rates of the two NiSi/Si interfaces in Figure 4a,b were not the same. When we consider the growth of the NiSi in Figure 1h, its growth has passed the point contact, and the Ni atoms must diffuse through the NiSi. The growth is found to be slow with an activation energy of 1.7 eV/atom, which is close to the value for NiSi growth in thin film silicide reactions.[28,32] Therefore, in point contact reaction, the nano-NiSi growth starts from both ends rather than from the point contact for three possible reasons. First, the supersaturation of Ni atoms at the point contact is impeded by the limited contact area and the oxide. Second, the ends of Si NWs are

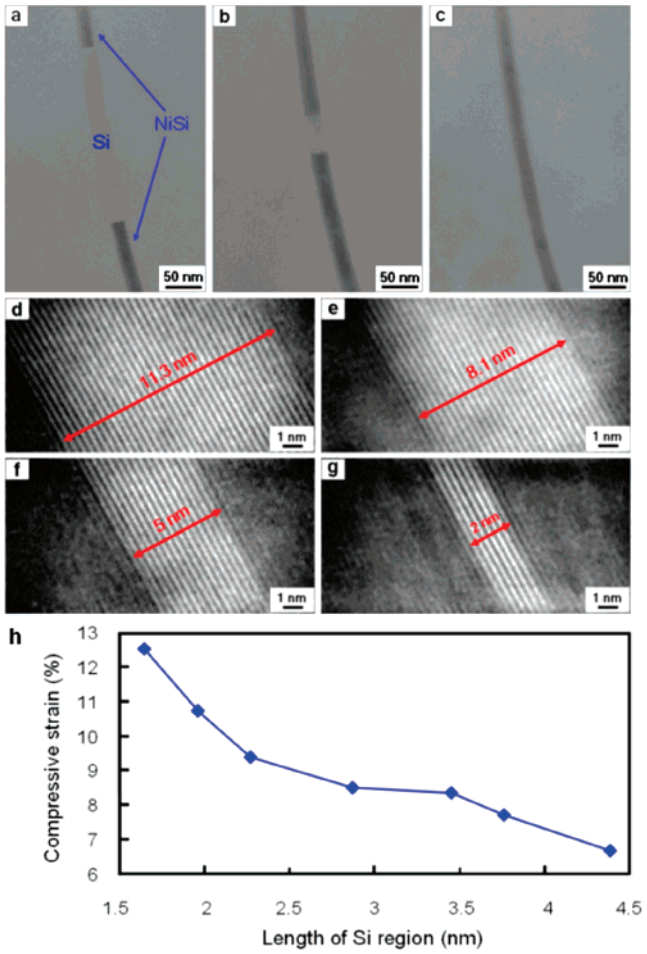

Figure 4. In situ TEM images showing the formation of our NiSi/Si/NiSi heterostructures within a Si nanowire and compressive strain in the Si region. **(**a,b) In situ TEM images of the NiSi/Si/NiSi heterostructure. The bright area is Si and the dark area is NiSi. (d−g) HRTEM images of NiSi/Si/NiSi heterostructures. The bright and dark portions of the lattice images correspond to Si and NiSi, respectively. (h) Plot of the compressive strain vs the length of the Si region in the nanoheterostructure NiSi/Si/NiSi.

considered to be favorable nucleation sites for the NiSi phase. Third, a chemical reaction tends to proceed along the pathway with lower activation energy. For interstitial diffusion within a Si nanowire, it is easier for Ni atoms to diffuse through Si with an activation energy of 1.25 eV/atom, leading to the growth from the ends, than through NiSi with activation energy of 1.7 eV/atom for the growth from the point contact. In other words, if the NiSi had started at the Ni NW−Si NW cross-point contact, it would have needed to diffuse through NiSi along a pathway with higher activation energy. It is worth mentioning that both of the two activation energies were measured in the present study. On the basis of the growth rates, we can control the remaining length of the Si region between the two NiSi regions, as illustrated in Figure 1h. We can pattern or deposit two Ni nanowires with a given spacing over a Si wire and then utilize the reaction to bring the two NiSi grains as close as possible. At 500 °C, the reaction rate can be controlled down to atomic scale as shown in Figure 2. In Figure 4d−g, a set of lattice images of the nanoheterostructure of NiSi/Si/NiSi with 11.3, 8.1, 5, and 2 nm lengths of Si is shown. By measuring the length of the Si region and counting the number of (111) lattice planes within the region, we can determine the strain, and we find that the Si is highly compressed. Figure 4h shows the relationship between the compressive strain and the length of the Si region in the nanoheterostructure NiSi/Si/NiSi at room temperature. In the process of NiSi formation, the diffusion of Ni atoms into Si lattice could have led to volume expansion. However, because of the confinement of the oxide on the Si nanowire, NiSi coming from both sides compressed the middle Si region, resulting in compressive stress on Si in the length direction. As a result, the strain increased when the length of the Si region decreased. The strain can be controlled because we can control the length of the Si region. Since one-dimensional nanoheterostructures may have potential applications in nanoelectronic devices,[5] the strain will affect carrier mobility in the Si region.

In conclusion, we have demonstrated the controlled growth of NiSi/Si/NiSi nanoheterostructures with the Si region as small as 2 nm in length through point contact reaction. In addition, it has been shown that the growth of single-crystal NiSi within a Si nanowire that starts from both ends attributed to the ease of nucleation and fast diffusion of Ni atoms in Si toward the ends. In situ TEM images demonstrate that the epitaxial growth of NiSi in Si nanowires is atomically flat. Direct evidence from in situ TEM videos shows that the single-crystal grains of NiSi have a linear growth rate and we propose that point contact reaction is limited by the rate of dissolution of Ni into Si at the point contact interface; in other words, we have demonstrated that the growth mechanism of NiSi in nanoscale is fundamentally different from that in thin films.[32] Controlled strain up to more than 12% in the Si region was observed. Also, from the growth rate we are able to control the formation of nanoheterostructures of silicide/Si/silicide to the nanometer or even atomic scale.

Acknowledgment. The authors would like to thank Professor Nosang V. Myung at UCR for the Ni nanowires and Professor Yu Huang at UCLA and Professor J. W. Mayer at ASU for helpful comments. The authors at NTHU would like to acknowledge the support by National Science Council through Grant NSC 95-2120-M-007-012 and Ministry of Education Grant 91-E-FA04-1-4.

Supporting Information Available: TEM videos of the growth of a single-crystal NiSi nanowire within a Si nanowire at 10 times the actual speed, the NiSi/Si epitaxial interface within a Si nanowire, the NiSi/Si epitaxial interface with a large step within a Si nanowire, and the two NiSi/Si epitaxial interfaces from both ends of a Si nanowire. This material is available free of charge via the Internet at http://pubs.acs.org.

References

(1) Cui, Y.; Lieber, C. M. *Science* **2001**, *291*, 851−853.
(2) Xia, Y.; Yang, P.; Sun, Y.; Wu, Y.; Mayers, B.; Gates, B.; Yin, Y.; Kim, F.; Yan, H. *Adv. Mater.* **2003**, *15*, 353−388.
(3) Patolsky, F.; Timko, B. P.; Zheng, G.; Lieber, C. M. *MRS Bull.* **2007**, *32*, 142−149.

(4) Wu, Y.; Xiang, J.; Yang, C.; Lu, W.; Lieber, C. M. *Nature* **2004**, *430*, 61−65.
(5) Weber, W. M.; Geelhaar, L.; Graham, A. P.; Unger, E.; Duesberg, G. S.; Liebau, M.; Pamler, W.; Cheze, C.; Riechert, H.; Lugli, P.; Kreupl, F. *Nano Lett.* **2006**, *6*, 2660−2666.
(6) Hsu, H. C.; Wu, W. W.; Hsu, H. F.; Chen, L. J. *Nano Lett.* **2007**, *7*, 885−889.
(7) Liu, B.; Wang, Y.; Dilts, S.; Mayer, T. S.; Mohney, S. E. *Nano Lett.* **2007**, *7*, 818−824.
(8) Chueh, Y. L.; Ko, M. T.; Chou, L. J.; Chen, L. J.; Wu, C. S.; Chen, C. D. *Nano Lett.* **2006**, *6*, 1637−1644.
(9) Schmitt, A. L.; Bierman, M. J.; Schmeisser, D.; Himpsel, F. J.; Jin, S. *Nano Lett.* **2006**, *6*, 1617−1621.
(10) Schmitt, A. L.; Zhu, L.; Schmeisser, D.; Himpsel, F. J.; Jin, S. *J. Phys. Chem. B* **2006**, *110*, 18142−18146.
(11) Song, Y.; Schmitt, A. L.; Jin, S. *Nano Lett.* **2007**, *7*, 965−969.
(12) Seo, K.; Varadwaj, K. S. K.; Mohanty, P.; Lee, S.; Jo, Y.; Jung, M. H.; Kim, J.; Kim, B. *Nano Lett.* **2007**, *7*, 1240−1245.
(13) Björk, B. T.; Ohlsson, B. J.; Sass, T.; Persson, A. I.; Thelander, C.; Magnusson, M. H.; Deppert, K.; Wallenberg, L. R.; Samuelson, L. *Appl. Phys. Lett.* **2002**, *80*, 1058−1060.
(14) Xiang, J.; Vidan, A.; Tinkham, M.; Westervelt, R. M.; Lieber, C. M. *Nat. Nanotechnol.* **2006**, *1*, 208−213.
(15) Wang, Z. L.; Ponchara, P.; de Heer, W. A. *Pure Appl. Chem.* **2000**, *72*, 209−219.
(16) Ross, F. M. *IBM J. Res. Dev.*. **2000**, *44*, 489−501.
(17) Stach, E. A.; Pauzauskie, P. J.; Kuykendall, T.; Goldberger, J.; He, R.; Yang, P. *Nano Lett.* **2003**, *3*, 867−869.
(18) Golberg, D.; Li, Y. B.; Mitome, M.; Bando, Y. *Chem. Phys. Lett.* **2005**, *409*, 75−80.
(19) Law, M.; Zhang, X. F.; Yu, R.; Kuykendall, T.; Yang, P. *Small* **2005**, *1*, 858−865.
(20) Liao, C. N.; Chen, K. C.; Wu, W. W.; Chen, L. J. *Appl. Phys. Lett.* **2005**, *87*, 141903-1-3.
(21) He, J. H.; Wu, W. W.; Chueh, Y. L.; Hsin, C. L.; Chen, L. J.; Chou, L. J. *Appl. Phys. Lett.* **2005**, *87*, 223102-1-3.
(22) Liu, C. H.; Wu, W. W.; Chen, L. J. *Appl. Phys. Lett.* **2006**, *88*, 023117-1-3.
(23) Liu, C. H.; Wu, W. W.; Chen, L. J. *Appl. Phys. Lett.* **2006**, *88*, 133112-1-3.
(24) Lang, C.; Kodambaka, S.; Ross, F. M.; Cockayne, D. J. H. *Phys. Rev. Lett.* **2006**, *97*, 226104-1-4.
(25) Leong, M.; Doris, B.; Kedzierski, J.; Rim, K.; Yang, M. *Science* **2004**, *306*, 2057−2060.
(26) He, R.; Yang, P. *Nat. Nanotechnol.* **2006**, *1*, 42−46.
(27) Nava, F.; Tu, K. N.; Bisi, O. *Mater. Sci. Rep.* **1993**, *9*, 141−200.
(28) Mayer, J. W.; Poate, J. M.; Tu, K. N. *Science* **1975**, *190*, 228−234.
(29) Tu, K. N. *Appl. Phys. Lett.* **1975**, *27*, 221−224.
(30) Foll, F.; Ho, P. S.; Tu, K. N. *J. Appl. Phys.* **1981**, *52*, 250−255.
(31) Chen, L. J.; Tu, K. N. *Mater. Sci. Rep.* **1991**, *6*, 53−140.
(32) Tu, K. N.; Mayer, J. W.; Feldman, L. C. *Electronic Thin Film Science*; Macmillian Publishing: New York, 1992.
(33) Chen, L. J. *JOM* **2005**, *57* (9), 24−30.
(34) Wagner, R. S.; Ellis, W. C. *Appl. Phys. Lett.* **1964**, *4*, 89−90.
(35) Hannon, J. B.; Kodambaka, S.; Ross, F. M.; Tromp, R. M. *Nature* **2006**, *440*, 69−71.
(36) Shingubara, S.; Okino, O.; Sayama, Y.; Sakaue, H.; Takahagi, T. *Solid-State Electron.* **1999**, *43*, 1143−1146.
(37) Spit, F. H. M.; Gupta, D.; Tu, K. N. *Phys. Rev. B* **1989**, *39*, 1255−1260.
(38) Weber, E. R. *Appl. Phys. A* **1983**, *30*, 1−22.
(39) Toman, K. *Acta Crystallogr.* **1951**, *4*, 462−464.
(40) Kästner, G.; Gösele, U. *Philos. Mag.* **2004**, *84*, 3803−3824.
(41) Thompson, R. D.; Gupta, D.; Tu, K. N. *Phys. Rev. B* **1985**, *33*, 2636−2641.

NL071046U